Spectroscopic investigation of the species involved in the rhodium-catalyzed oxidative carbonylation of toluene to toluic acid†

Joseph Zakzeski,[a] Sarah Burton,[b] Andrew Behn,[a] Martin Head-Gordon[c] and Alexis T. Bell*[a]

Received 6th April 2009, Accepted 27th July 2009
First published as an Advance Article on the web 21st August 2009
DOI: 10.1039/b906883j

A spectroscopic investigation of complexes used to catalyze the oxidative carbonylation of toluene to *p*-toluic acid was conducted. Rhodium complexes were analyzed by ^{103}Rh and ^{13}C NMR, UV-visible spectroscopy, and infrared spectroscopy. In the presence of vanadium and oxygen, the resting state of the Rh-catalyst was found to exist as a Rh(III) complex with carbonyl and trifluoroacetate ligands, consistent with the structure $Rh(CO)_2(TFA)_3$. The ^{13}C NMR spectrum of $Rh(^{13}CO)_2(TFA)_3$ complex exhibited a carbonyl peak with an unusual degree of shielding, which resulted in the appearance of the carbonyl peak at an unprecedented upfield position in the ^{13}C NMR spectrum. This shielding was caused by interaction of the carbonyl group with the trifluoroacetate ligand. In the absence of oxygen, the Rh(III) complex reduced to Rh(I), and the reduced form exhibited properties resembling the catalyst precursor. Structures and spectroscopic properties calculated using density functional theory agreed closely with the experimental results. The vanadium co-catalyst used to reoxidize Rh(I) to Rh(III) was similarly characterized by ^{51}V NMR and UV-visible spectroscopy. The oxidized species corresponded to $[(VO_2)(TFA)]_2$, whereas the reduced species corresponded to $(VO)(TFA)_2$. The spectroscopic results obtained in this study confirm the identity of the species that have been proposed to be involved in the Rh-catalyzed oxidative carbonylation of toluene to toluic acid.

1. Introduction

The oxidative carbonylation of toluene represents a potentially useful route to synthesize *p*-toluic acid, which is an intermediate used in the production of terephthalic acid. Terephthalic acid reacts with ethylene glycol to form polyethylene terephthalate (PET), a compound used extensively in plastics and resins.

Several studies have demonstrated that *p*-toluic acid can be synthesized by oxidative carbonylation of toluene catalyzed by Rh(III) cations in the presence of trifluoroacetic acid (TFAH) and its anhydride (TFAA) together with a vanadium oxo co-catalyst and molecular oxygen.[1,2] The active center in this system is thought to be $Rh(CO)_x(TFA)_3$ ($x = 1$ or 2).[1–4] Kalinovskii and co-workers have proposed that $Rh(CO)_x(TFA)_3$ reacts with toluene to form an aryl–rhodium complex $Rh(CO)(TFA)_3(Ph)$.[3] Migratory insertion of CO into the arene–metal bond forms $PhCO–Rh(TFA)_3$, which then undergoes reductive elimination to form the mixed anhydride of toluic and trifluoroacetic acids.[3] Upon release of this product, the Rh cation is reduced from Rh(III) to Rh(I). The VO_x species in the reaction mixture then oxidize Rh(I) back to Rh(III). The basic features of this mechanism have been supported by subsequent experimental work carried out by Zakzeski and Bell[2] and theoretical work reported by Zheng and Bell.[5] The results of these studies indicated that the resting state of the catalyst is most likely to be $Rh(CO)_2(TFA)_3$, a structure satisfying the 18-electron rule, and that the overall reaction mechanism is that shown in Scheme 1. This scheme also provides a detailed picture of the mechanism by which Rh(I) is reoxidized to Rh(III) by VO_2^+ cations and the mechanism by which O_2 participates in the reoxidation of VO^{2+} cations to VO_2^+ cations. While Scheme 1 captures all of the features of the reaction system observed experimentally, to the best of our knowledge, little experimental evidence exists to support the structures and identities of the rhodium and vanadium complexes present in the proposed catalytic cycles. The objective of this investigation was to obtain direct spectroscopic evidence for these complexes, namely $Rh(CO)_2(TFA)_3$, $Rh(CO)_2(TFA)$, VO_2TFA and $VO(TFA)_2$, using infrared, UV-visible, and ^{13}C and ^{103}Rh NMR spectroscopy.

2. Experimental

$[Rh(CO)_2Cl]_2$ (Alfa Aesar), the precursor to the active form of the catalyst, and NH_4VO_3 (Aldrich, 99 + %), the precursor to the oxidant used to reoxidize Rh(I) to Rh(III), were dissolved in a mixture of trifluoroacetic acid (TFAH) (Aldrich, 99%), trifluoroacetic anhydride (TFAA) ($\geq$ 99%, Aldrich), and

[a] *Department of Chemical Engineering, University of California, Berkeley, CA 94720-1462, USA. E-mail: bell@cchem.berkeley.edu; Fax: +1 1-510-642-4778; Tel: +1 1-510-642-1536*
[b] *Environmental Molecular Sciences Laboratory, Pacific Northwest National Laboratory, 3335 Q Avenue, Mail-Stop K8-98, Richland, WA 99354, USA*
[c] *Department of Chemistry, University of California, Berkeley, CA 94720-1460, USA*

† Electronic supplementary information (ESI) available: Nuclear coordinates, energies, and Gibbs free energies for Rh and V species and solution infrared spectra following reaction. See DOI: 10.1039/b906883j

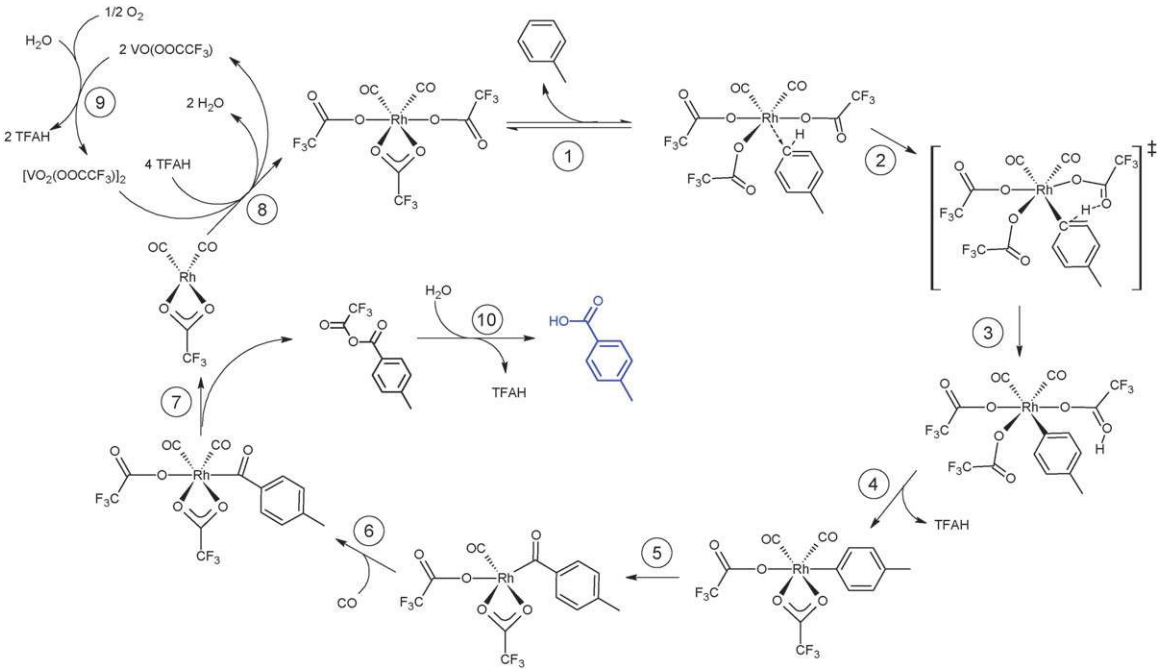

Scheme 1 Proposed mechanism for Rh- and V-catalyzed toluene oxidative carbonylation as indicated by ref. 2 and 5. See ref. 29 for the geometry of the transition state.

toluene (99.8%, Aldrich). Room temperature experiments were conducted in glass vials, whereas high temperature and pressure reactions were conducted in stirred, 50 mL Parr autoclaves made of Hastelloy C. Between runs, each type of reactor was washed thoroughly with water and acetone and then dried in a vacuum oven overnight to avoid contamination. The reaction temperature in the autoclaves was monitored using a thermocouple placed in a Hastelloy C thermowell. The autoclave headspace was purged four times with helium. After purging, the autoclave was pressurized at 293 K with 0.345 MPa O_2 (99.993%, Praxair) and 0.345 MPa CO (99.5%, Praxair).

^{13}C NMR experiments carried out by placing the solution of interest in a Wilmad Labglass, high-pressure NMR tube, and then pressurizing the tube to 0.345 MPa with ^{13}CO (Isotec, min 99% ^{13}CO). The tube was then inverted several times to enhance mixing. ^{13}C NMR measurements were made on a Bruker DRX-500 or a Bruker AV-600 spectrometer without lock using a 5 mm ZBO probe with proton decoupling. Chemical shifts were assigned relative to the methyl peak of toluene at 20.4(7) ppm. ^{19}F NMR spectra were obtained on a Bruker AVQ-400 using a standard glass NMR tube with D_2O contained in a capillary tube as the lock source. Chemical shifts were measured relative to $CFCl_3$ at 0 ppm. ^{51}V NMR measurements were conducted on a Bruker AVB-400 spectrometer using a standard glass NMR tube with D_2O in a capillary tube as a lock source. Chemical shifts in this case were referenced to $VOCl_3$ at 0 ppm. ^{103}Rh NMR measurements were obtained on a 499.803 MHz Varian Unity+ spectrometer equipped with a Varian 10 mm HX probe. The frequencies used for the ^{103}Rh transmitter frequencies ranged from 15.7 to 15.9 MHz. The $\delta(^{103}Rh)$ values were calculated by determining the absolute frequency of the cross peak and relating it to the arbitrary reference frequency (Ξ = 3.16 MHz at 100.00 MHz), which is 15.800 for operation at 500 MHz. Since the operating frequency of 499.803 MHz differed from 500 MHz, a 394.4 ppm correction was added to all ^{103}Rh chemical shifts. Analysis of a sample of $Rh(acac)_3$ and $[Rh(CO)_2Cl]_2$ resulted in peaks at 8349 and 118 ppm, respectively, in good agreement with literature values of 8358 for $Rh(acac)_3$ and 84 for $[Rh(CO)_2Cl]_2$.[6] For analysis by ^{103}Rh NMR, the solutions were concentrated to 0.1 M Rh and analyzed in 10 mm diameter tubes to aid in detection.

UV-visible spectroscopy was conducted using a Varian Cary 400 Bio UV-visible spectrophotometer. Solutions were placed in 10 mm standard quartz spectroscopic cells and analyzed from 900 to 300 nm with a scan rate of 600 nm min^{-1}. The solvent, typically a mixture of toluene, trifluoroacetic acid, and trifluoroacetic anhydride, was used for baseline correction.

IR spectroscopy measurements were conducted using a Nicolet 6700 FT-IR equipped with a demountable liquid cell (Harrick, Inc.), which is equipped with 13 mm CaF_2 windows. Analyses were made by transferring the liquid contained in an autoclave to the demountable liquid cell and immediately acquiring a spectrum. Baseline correction was conducted using a mixture of toluene, trifluoroacetic acid, and trifluoroacetic anhydride.

3. Theoretical

Computed structures, normal modes, and NMR shifts were determined using density functional theory (DFT) as implemented in Q-Chem.[7] Geometry optimizations and vibrational analyses were performed using the B3LYP density functional with the 6-31G* basis set applied to all atoms

except rhodium which was described by the LANL2DZ pseudopotential.[8–10] Vibrational frequencies were scaled by 0.9614 to correct for systematic overestimation.[11] Calculated energies were refined with the 6-311G** basis set for all non-rhodium atoms. NMR shifts were calculated using the Hartree–Fock wavefunction of the B3LYP equilibrium geometry, and rhodium was described using the all electron 3-21G basis set. To correct for the systematic overestimation of NMR shifts, a small library of rhodium carbonyl shifts were calculated (compounds and theoretical shifts in ppm: $Rh(Py)(CO)_2Cl$, 185.6 and 181.3; $Rh(Acac)(CO)_2$, 183.8; $Rh(Acac)(Ph_3P)CO$, 190.4; and $Rh(\eta_5\text{-}C_5H_5)(CO)_2$, 190.9) and compared to published experimental values.[12] The mean and standard deviation of the theoretical–experimental offset was found to be 65 ± 8 ppm. This value was then used as a general correction to our calculations.

4. Results and discussion

Analysis of the solvent in the absence of Rh or V species was conducted in order to establish a background for each analytical method. A mixture consisting of toluene, trifluoroacetic acid, and trifluoroacetic anhydride did not exhibit UV-visible bands in the range 900 to 300 nm. When a portion of this mixture was placed in a high-pressure NMR tube and exposed to 0.35 MPa ^{13}CO, a carbonyl peak associated with free CO appeared at 184 ppm.[13] Peaks from the solvent were also clearly identifiable: two quartets attributable to trifluoroacetic acid were observed at 160.8 and 114.2 ppm, and two quartets attributable to trifluoroacetic anhydride were observed at 149.2 and 113.0 ppm. In addition, strong peaks associated with the toluene solvent were observed at 137.5, 128.7, 127.9, and 125.0, and 20.5 ppm. The IR spectrum of the solution exhibited strong absorbances in the range of 1950–500 cm^{-1} characteristic of trifluoroacetic acid, trifluoroacetic anhydride, and toluene.

Dissolution of NH_4VO_3 in a mixture of trifluoroacetic acid and trifluoroacetic anhydride produced an orange-colored solution, which exhibited a ligand-to-metal charge transfer band below 300 nm, but no bands were observable in the visible region. When toluene was added to this solution, it turned orange/brown in color and new transitions appeared at 410 and 455 nm, which are discussed later. When this sample was pressurized to 0.35 MPa ^{13}CO, a ^{13}C NMR peak associated with free CO, was observed at 184 ppm; however, neither ^{13}C NMR nor IR spectroscopy showed any evidence for carbonyl groups associated with the dissolved V(v) species. These results suggest that vanadium–carbonyl complexes do not form under the conditions used to obtain the spectroscopic data.

$[Rh(CO)_2Cl]_2$, the catalyst precursor used in these studies, was characterized after dissolving it in a solution containing trifluoroacetic acid, trifluoroacetic anhydride, and toluene. Analysis of this solution by ^{103}Rh NMR resulted in a single peak at 118 ppm, which lies in the range expected for Rh(I) complexes.[14] ^{13}C NMR analysis of this solution after pressurization with 0.35 MPa ^{13}CO produced a doublet at 177.8 and 177.2 ppm ($J_{^{103}Rh-^{13}C}$ = 76.7 Hz) attributable to a Rh(I) carbonyl peaks.[15] The infrared spectrum of the solution taken in the absence of ^{13}CO exhibited strong carbonyl stretches at 2090 and 2034 cm^{-1}, and a weaker carbonyl feature at 2107 cm^{-1}. The UV-visible spectrum of the resulting yellow-colored solution showed no bands in the region of 900 to 500 nm and only a peak at 325 nm. The observed ^{13}C chemical shift and the ^{103}Rh–^{13}C coupling constant agree very closely with the values reported for $[Rh(CO)_2Cl]_2$ dissolved in CD_2Cl_2, ($\delta(^{13}C)$: 178.3 ppm, $J_{^{103}Rh-^{13}C}$: 76.9 Hz).[16] There is also close agreement between the observed IR bands and those seen for $[Rh(CO)_2Cl]_2$.[16] The strong bands are associated with a B_1 and B_2 stretch of the carbonyl groups, and the weak band is associated with an A_1 stretch. These stretches arise because the complex, a d^8 square-planar Rh dimer complex, adopts a C_{2v} symmetry point group because of bending at the bridging chlorine atoms.[16] Taken together, our observations indicate that the catalyst precursor, $[Rh(CO)_2Cl]_2$, does not undergo reaction upon room-temperature dissolution in the reaction mixture.

The oxidative carbonylation of toluene was conducted under the reaction conditions described in the Experimental section for 0.5 h, after which the reaction mixture was analyzed at room temperature to identify Rh species present. The color of the solution after reaction was emerald-green/brown as compared to yellow prior to reaction and a peak appeared at 600 nm in the UV-visible spectrum characteristic of Rh(III) cations. The presence of Rh(III) was also confirmed by ^{103}Rh NMR, which showed a single peak at 6322 ppm characteristic of a Rh(III) complex[14] with a relatively deshielded metal center. Pressurization of the reaction mixture with 0.35 MPa ^{13}CO and subsequent ^{13}C NMR showed carbonyl peaks broadened extensively by the presence of a high concentration of paramagnetic and quadrupolar V(IV) species (see below). Therefore, a second 0.5 h reaction was conducted with a lower concentration of vanadium (approximately 24 μmol mL^{-1}). The full ^{13}C NMR spectrum is presented in Fig. 1a and the region between 140 and 120 ppm is presented in Fig. 1b. A doublet attributable to a carbonyl species was observed at 130.0 ppm ($J_{^{103}Rh-^{13}C}$ = 194.8 Hz), a shift not typically characteristic for Rh(I) or Rh(III) carbonyls.[17] To ascertain that the new ^{13}C peaks were not due to organic species, a proton-coupled spectrum was acquired. Neither peak-splitting nor shift was observed in the proton-coupled spectrum, consistent with the assignment of these peaks to rhodium–carbonyl groups. Moreover, no peaks were observed in the absence of Rh or ^{13}CO. To rule out the possibility that the new ^{13}C NMR peaks might be due to CO_2, the liquid was pressurized with $^{13}CO_2$. This led to the observation of a peak at 124.5 ppm. Analysis of the isotopically unlabeled solution by infrared spectroscopy with higher vanadium concentrations (approximately 93 μmol mL^{-1}) revealed two strong peaks of roughly equal intensity at 1714 and 1684 cm^{-1} and two weak peaks at 2122 and 2113 cm^{-1}. In the absence of CO, no significant peaks occur above 1600 cm^{-1}. The UV-visible spectrum of the reaction solution containing CO, which was an emerald-green/brown color, is shown in Fig. 2a. The UV-visible spectrum exhibits broad, overlapping bands at 317, 410, 455, and 600 nm.

The evidence presented above shows that after 0.5 h of reaction all trace of $[Rh(CO)_2Cl]_2$ have disappeared and,

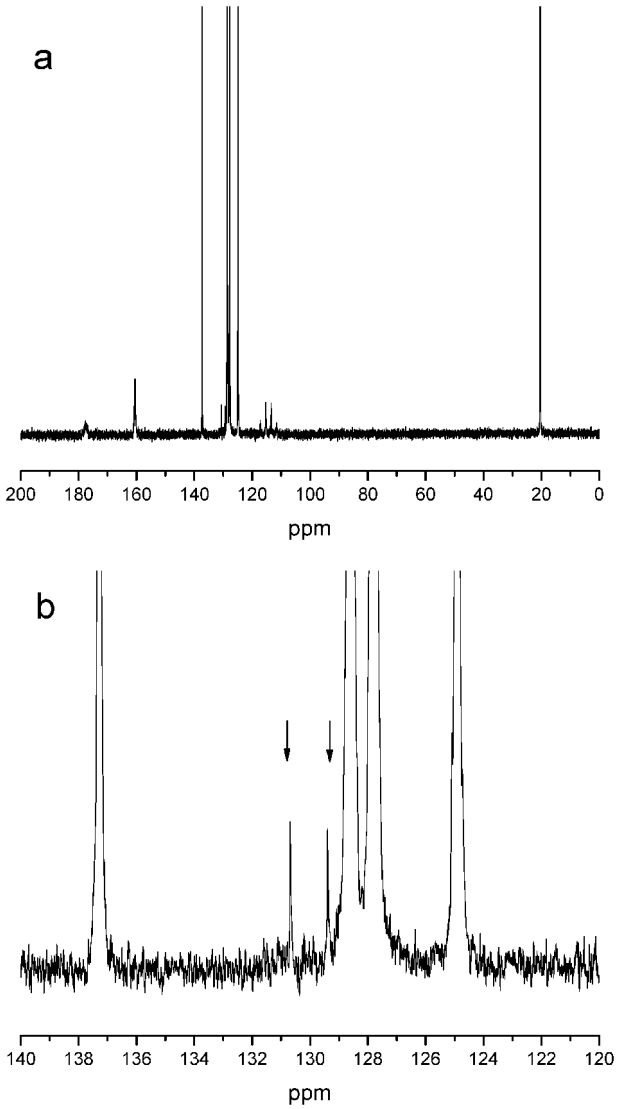

Fig. 1 (a) Full ^{13}C NMR spectrum (0–200 ppm) of the reaction solution. (b) View of spectrum from 120 to 140 ppm. Toluene (12.4 mmol), trifluoroacetic acid (4.2 mmol), and trifluoroacetic anhydride (1.3 mmol), $[Rh(CO)_2Cl]_2$ (14.4 μmol), NH_4VO_3 (44 μmol), 0.345 MPa O_2, 0.345 MPa CO, T = 353 K, t = 1/2 h.

hence, all of the Rh(I) complex was oxidized to a Rh(III) complex in the course of reaction. Of further note, the position of the ^{103}Rh NMR peak suggests that the cation is highly deshielded, as would occur if the Rh(III) cations were coordinated with highly electron withdrawing anions, such as trifluoroacetate. The coordination of CO with Rh(III) is clearly indicated by the data obtained from ^{13}C NMR and IR; however, the ^{13}C chemical shift of coordinated ^{13}CO is uncharacteristic for terminal rhodium carbonyls. The infrared bands at 1684 and 1714 cm^{-1} are consistent with CO vibrations within a unidentate trifluoroacetate ligand. The observation of two bands is consistent with the structure of $Rh(CO)_2(TFA)_3$, which possesses one bidentate and two unidentate trifluoroacetate ligands. In the absence of CO these peaks are not observed for $Rh(TFA)_3$, which does not contain bidentate ligands. As discussed below, the unusual ^{13}C NMR and IR

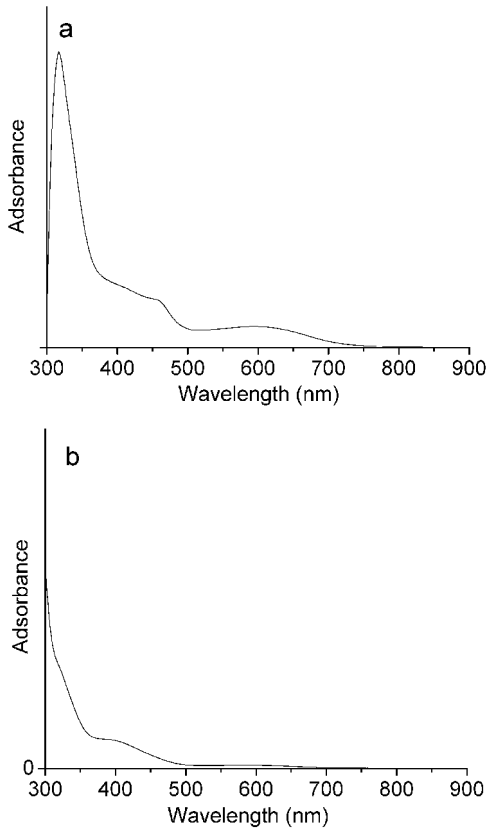

Fig. 2 (a) Reaction solution after 1/2 hour. Toluene (12.4 mmol), trifluoroacetic acid (4.2 mmol), and trifluoroacetic anhydride (1.3 mmol), $[Rh(CO)_2Cl]_2$ (5 μmol), NH_4VO_3 (170 μmol), 0.345 MPa O_2, 0.345 MPa CO, T = 353 K, t = 1/2 h. (b) Reaction solution after exposure to CO for 3 hours. 0.345 MPa CO, T = 353 K, t = 3 h.

characteristics of the CO ligands can be attributed to interaction of the carbonyl groups with the trifluoroacetate ligands coordinated with the Rh(III) cation.

The two very small IR peaks of roughly equal intensity detected at 2122 and 2113 cm^{-1} are likely due to the decomposition of the Rh(III) dicarbonyl complex to two monocarbonyl isomers. In fact, loss of CO was evident by the decrease in intensity of both IR carbonyl signals and the ^{13}C NMR peaks with time when the complex was not under CO pressure. Under CO pressure, however, the dicarbonyl–rhodium complex was stable. Because the NMR spectra were recorded using a pressurizable NMR tube under a ^{13}CO atmosphere, the dicarbonyl species was stable, and there was no evidence for a Rh(III) monocarbonyl species under these conditions.

As shown in Scheme 1, the Rh (III) complex assumed to be active for the activation of toluene and its subsequent oxidative carbonylation to toluic acid undergoes reduction to Rh(I) at the end of the reaction sequence. The mechanism presented in Scheme 1 suggests that in the absence of O_2, needed to reoxidize the vanadium species involved in the oxidation of Rh(I) to Rh(III), all of the Rh will accumulate in the Rh(I) state. The following experiments were, therefore, conducted in order to characterize the Rh(I) complex. After 0.5 h of reaction the autoclave headspace was flushed free of O_2 using dry He, repressurized with CO, and the reaction was

then continued for an additional hour. The resulting solution was light green/yellow in color. ^{13}C NMR analysis of the solution after pressurizing it with ^{13}CO revealed a broad doublet at 177.2 ppm. To obtain better ^{13}C NMR spectra, the experiment was repeated with a higher Rh loading (120 μmol mL^{-1}) and the reduction in the presence of CO (and the absence of O_2) was conducted for 3 h. Fig. 3 shows the resulting ^{13}C NMR spectrum. A doublet was again observed at 177.2 ppm ($J_{^{103}Rh-^{13}C}$ = 79.2 Hz). The IR spectrum of the solution exhibited a weak band at 2106, and strong bands at 2090 and 2033 cm^{-1}. Comparison of this UV-visible spectrum (Fig. 2b) with the spectrum taken after 0.5 h of reaction in the presence of CO and O_2 (Fig. 2a) showed that the reaction in CO alone resulted in the disappearance of the absorption band near 600 nm attributed to Rh(III) cations and a reduction in the intensities of the bands appearing below 500 nm. The ^{13}C NMR and IR spectra of the complex strongly resemble those of the $[Rh(CO)_2Cl]_2$ precursor (see above), suggesting that the Rh(I) species reverts to the chlorine-bridged dimer upon reduction; however, it is also possible that the Rh(I) cations are now present as $[Rh(CO)_2TFA]_2$ complexes or a combination of this complex and $[Rh(CO)_2Cl]_2$. These alternatives are discussed more fully below.

Density functional theory calculations were conducted in order to aid in interpretation of the experimental results obtained under reaction conditions and presented in the preceding paragraphs. Earlier DFT calculations reported by Zheng and Bell[5] have suggested that the active form of Rh(III) under the conditions used in the present study is $Rh(CO)_2(TFA)_3$. Additional analysis of this complex was undertaken in the course of the present investigation with the aim of establishing whether the experimentally observed characteristics of the Rh(III) complex reported here are consistent with the assignment of this complex as $Rh(CO)_2(TFA)_3$.

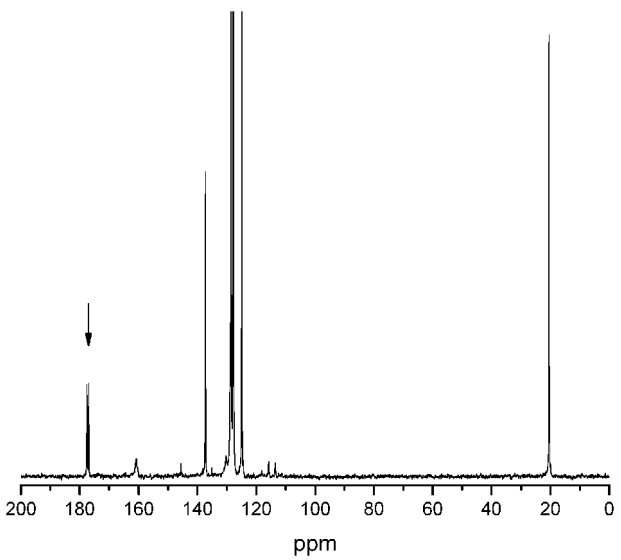

Fig. 3 ^{13}C NMR spectra of Rh, the reaction solution after 3 h in the absence of O_2. Toluene (49.5 mmol), trifluoroacetic acid (17.2 mmol), and trifluoroacetic anhydride (4.9 mmol), $[Rh(CO)_2Cl]_2$ (219.7 μmol), NH_4VO_3 (1 mmol), 0.345 MPa CO, T = 353 K, t = 3 h.

Fig. 4a depicts the optimized geometry of the lowest energy isomer of $Rh(CO)_2(TFA)_3$, assuming that it is in the gas phase. The other two isomers (not shown) possess *trans* carbonyls out of plane with the bidentate acetate, and *cis* carbonyls in plane with the bidentate acetate. The lowest energy isomer (shown) is the species of interest and adopts a pseudo-octahedral configuration with two *cis*-located carbonyls, one axial and one equatorial, relative to the plane of the bidentate trifluoroacetate. One of the three trifluoroacetate ligands differs significantly from the others by bonding with Rh *via* both the O1 and O2 atoms, whereas the remaining two trifluoroacetate ligands bond to Rh through a single oxygen atom (O3 and O5, respectively). It is noted that the carbonyl ligands display a large degree of angular distortion relative to most terminal carbonyl ligands. The angle between the first carbonyl and the Rh (O7–C3–Rh1) is approximately 137 degrees, whereas Rh–C–O bond angles of approximately 180 degrees are usually observed. The origin of this distortion is the close interaction between the carbonyl ligand and the trifluoroacetate bound to Rh by a single oxygen atom. Indeed, the distance between the O4 oxygen atom of the trifluoroacetate and the C3 carbon atom of the carbonyl is unusually short, only 0.153 nm, which closely resembles the C1–O4 distance of 0.130 nm found in the trifluoroacetate ligand itself. These factors, taken together, suggest that a bonding interaction occurs between the carbonyl ligand and the trifluoroacetate ligand to form a five-membered ester-resembling ring with the Rh metal center. Since acetate ligands normally act as versatile bridging ligands,[18,19] this interaction stabilizes the trifluoroacetate ligands in the complex and significantly alters the electronic and vibrational characteristics of the carbonyl. A similar interaction is also observed between the second trifluoroacetate ligand and the second carbonyl ligand, but the extent to which the interaction occurs is reduced, as indicated by the Rh1–C4–O8 angle of approximately 165 degrees and a C4–O8 bond distance of 0.234 nm.

The ^{13}C NMR chemical shift for the carbonyl groups present in $Rh(CO)_2(TFA)_3$ was determined and then adjusted downwards by 65 ± 8 ppm to account for a systematic overprediction of the shift relative to measured ^{13}C shifts for various Rh carbonyls. The corrected calculated chemical shift for C3 is 134.6 ± 8 ppm and that for C4 is 164.7 ± 8 ppm. The corresponding IR frequencies for the C3–O and the C4–O bonds calculated with standard correction are 1893 and 2121 cm^{-1}, respectively. We note that the CO ligand that exhibits the unusually low ^{13}C NMR shift and low C–O vibrational frequency is the one that interacts with one of the trifluoroacetate ligands. This type of inter-ligand interaction is similar to that reported by Chetcuti and co-workers for Rh–aryl nitrile N-oxide complexes.[20] The crystal structure of this complex clearly shows that the carbonyl group interacts with the aryl nitrile N-oxide ligand in a manner very similar to that found in the calculations for $Rh(CO)_2(TFA)_3$ (see Fig. 5). Furthermore, the strong interaction of the CO ligand in Rh–aryl nitrile N-oxide complexes with the aryl nitrile N-oxide ligand causes a red-shift in the C–O stretching frequency to between 1700 and 1640 cm^{-1}.

In contrast to the ^{13}C NMR shifts calculated for $Rh(CO)_2(TFA)_3$, the experimental results show only a single

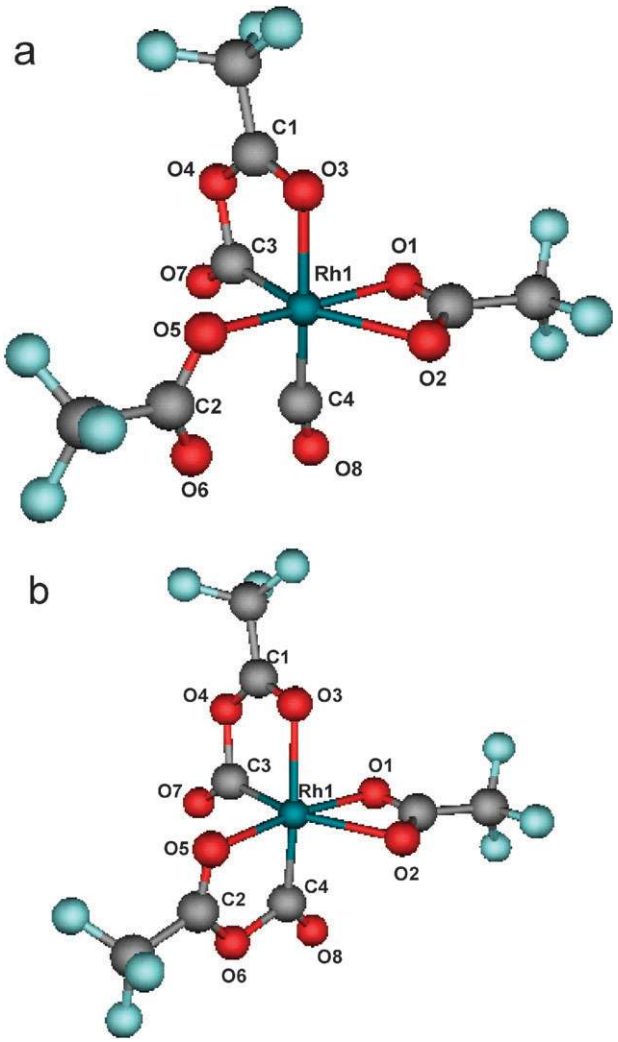

Fig. 4 (a) Computed geometry for the $Rh(CO)_2(TFA)_3$ complex. (b) Computed geometry for $Rh(CO)_2(TFA)_3$ showing the interaction of both carbonyl ligands with trifluoroacetate ligands.

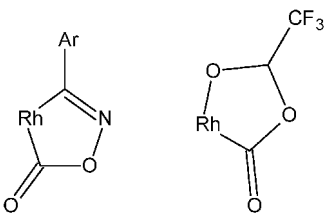

Fig. 5 Comparison of structures of Rh(CO)(TFA) interaction with Rh(CO)(C(Ar)NO) interaction proposed by Chetcuti and co-workers.[17] Extraneous ligands were omitted for clarity.

^{13}CO peak at 130.0 ppm. The absence of a ^{13}C NMR peak near 165 ppm suggests that both CO ligands interact with the trifluoroacetate ligands. By separately constraining the carbonyl–acetate interaction distance for each pair (O4–C3 and O6–C4) ^{13}C NMR shifts for each carbonyl ligand were computed over a range of interaction distances. These shifts (see Fig. 6) were found to be almost entirely a function of interaction distance, rather than of placement of CO in the complex (axial or equatorial). Based on this information, a

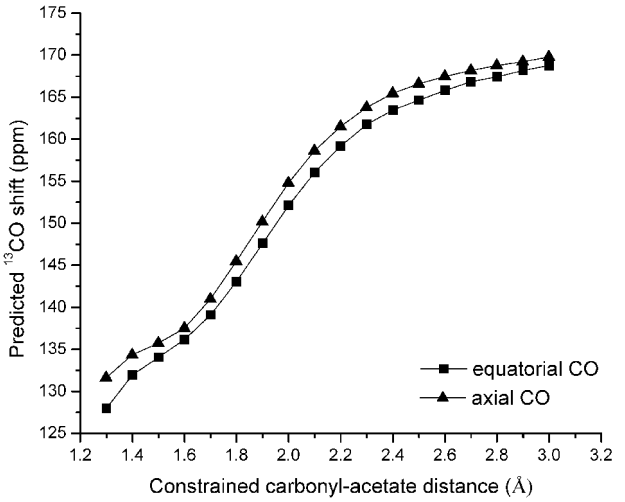

Fig. 6 Computed ^{13}C NMR chemical shifts as a function of constrained carbonyl–acetate distance for axial and equatorial CO.

proposed structure for $Rh(TFA)_3(CO)_2$ is shown in Fig. 4b, for the case in which both CO ligands exhibit identical ^{13}C NMR shifts at 130.0 ppm. This configuration of the complex shown in Fig. 4b does not represent an equilibrium structure of this complex, since calculations were made assuming that the complex was in the gas phase. It is possible, however, that specific solvent interactions, which cannot be handled because of excessive computational cost, stabilize the structure of the complex shown in Fig. 4b when it is in the liquid phase.

Additional DFT analysis was conducted to aid in characterization of the rhodium complex observed after reduction of the Rh(III) complex to a Rh(I) complex. The DFT calculations of Zheng and Bell[5] and those carried out in the context of the present study suggest that the Rh(I) complex is $Rh(CO)_2(TFA)$, a 16-electron, d^8 complex with a pseudo-square-planar geometry, in which the two carbonyl groups are *cis*-coordinated and the trifluoroacetate ligand is bonded to Rh by both oxygen atoms. As noted above, the experimental evidence indicates that the stable form of the Rh(I) complex exists as a dimer and consequently calculations were carried out for both $[Rh(CO)_2(TFA)]_2$ and the catalyst precursor, $[Rh(CO)_2Cl]_2$.

Fig. 7 depicts the calculated structure for $[Rh(CO)_2(TFA)]_2$. The calculated ^{13}C chemical shift for $[Rh(CO)_2(TFA)]_2$ after correction is 184 ± 8 ppm, and the calculated IR frequencies are 2102, 2085, and 2049 cm^{-1}, whereas the calculated ^{13}C chemical shift for $[Rh(CO)_2Cl]_2$ after correction is 182 ± 8 ppm, and the calculated IR frequencies are 2101, 2089, and 2045 cm^{-1}. These calculated values are to be compared with the experimentally observed ^{13}C carbonyl shift for the Rh(I) complex of 177.2 ppm, and observed IR frequencies of carbonyl stretching of 2106, 2090, and 2033 cm^{-1}. The closeness of the observed ^{13}C shifts and the IR band frequencies to those calculated for $[Rh(CO)_2(TFA)]_2$ and $[Rh(CO)_2Cl]_2$ makes it impossible to say unambiguously whether one or both of these species are present once the active catalyst has been reduced from the Rh(III) to the Rh(I) state.

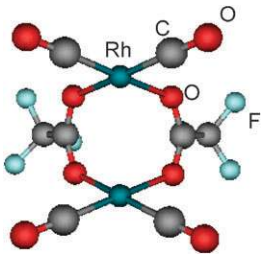

Fig. 7 Computed geometry for $[Rh(CO)_2(TFA)]_2$.

Additional calculations were carried out to determine the thermodynamics of converting $[Rh(CO)_2Cl]_2$ to $[Rh(CO)_2(TFA)]_2$ *via* the reaction:

$$[Rh(CO)_2Cl]_2 + 2TFAH \leftrightharpoons [Rh(CO)_2(TFA)]_2 + 2HCl \quad (1)$$

The Gibbs free energy change for this process at 298 K is +13 kcal mol^{-1}, which suggests that for a TFAH/Cl ratio of concentrations of approximately 2000 $[Rh(CO)_2Cl]_2$ would be favored by about 8 to 1 over $[Rh(CO)_2(TFA)]_2$. The thermodynamics for dissociating the dimeric species $[Rh(CO)_2(TFA)]_2$ to the monomeric species $Rh(CO)_2(TFA)$ was also examined. The Gibbs free energy change for the reaction:

$$[Rh(CO)_2(TFA)]_2 \leftrightharpoons 2Rh(CO)_2(TFA) \quad (2)$$

was found to be approximately +15 kcal mol^{-1}, indicating that formation of the monomeric species is highly unfavorable. However, in the presence of the oxidizing species (see Scheme 1), the Rh(I) complex is converted completely to the Rh(III) complex as shown by the experimental evidence presented above.

The identity of the vanadium complexes formed in solution was investigated in the following manner. NH_4VO_3 was dissolved in trifluoroacetic acid and the resulting orange-colored solution was then dried in a vacuum oven to yield an orange-colored powder. This product was then dissolved in D_2O and analyzed by ^{51}V and ^{19}F NMR. The results are depicted in Fig. 8a and Fig. 8b, respectively. The chemical shift of the vanadium species, which appeared at −545 ppm, is assigned to VO_2^+ species.[21] A strong fluorine peak was observed at −75 ppm characteristic of trifluoroacetate anions.[22,23] Taken together, these results suggest that the NH_4VO_3 reacts with trifluoroacetic acid to form the vanadium species $(VO_2)(TFA)$ *via* the following reaction:

$$NH_4VO_3 + TFAH \rightarrow (VO_2)(TFA) + NH_3 + H_2O$$

As indicated above, when a sample of this vanadium complex was added to toluene, a color change occurred associated with the appearance of two peaks at 410 and 455 nm in the UV-visible spectrum. Analysis of the toluene phase by GC/MS indicated trace quantities of toluene oxidation products, such as benzaldehyde and the ester of benzyl alcohol and trifluoroacetic acid, suggesting that the observed color change from yellow to orange/brown is associated with the reduction of the V(V) species to V(IV) species, a process known to occur with vanadyl compounds and arenes.[24] In the presence of water,

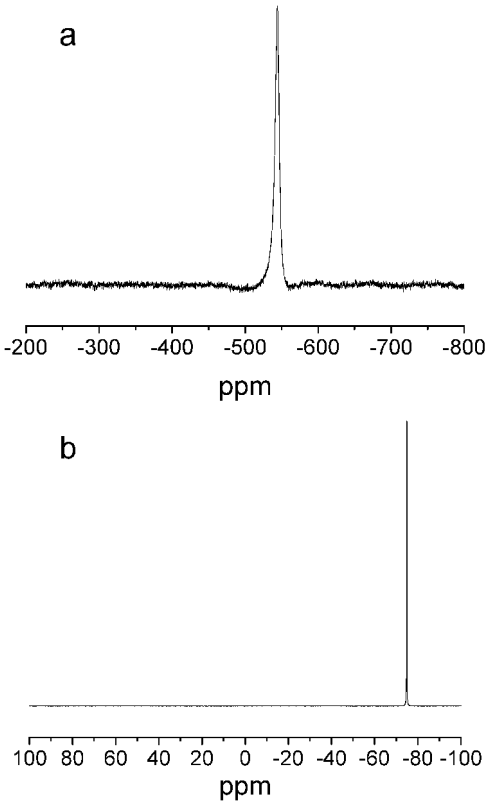

Fig. 8 0.138 mmol NH_4VO_3, 26.2 mmol TFAH. (a) ^{51}V NMR spectrum of $(VO_2)(TFA)$dissolved in D_2O. (b) ^{19}F NMR spectrum of $(VO_2)(TFA)$ dissolved in D_2O.

$(VO_2)(TFA)$ dissociates to form VO_2^+ and TFA^-, as suggested by the chemical shifts observed in the ^{51}V and ^{19}F NMR spectra. In the presence of toluene, trifluoroacetic acid, and trifluoroacetic anhydride, $(VO_2)(TFA)$ is most likely present as cation–anion pair because of the low dielectric constant of the solution. Our DFT calculations show that the stable form of this ion pair is a dimer, $[(VO_2)(TFA)]_2$, rather than a monomer, as shown in Fig. 9a. This complex resembles vanadium (V) complexes, which have been shown to form stable 5-coordinate dimeric species.[25]

The V complexes present during the oxidation of Rh(I) to Rh(III) were analyzed by ^{51}V NMR. Fig. 10 depicts the results of ^{51}V NMR of NH_4VO_3 dissolved in toluene, trifluoroacetic acid, and trifluoroacetic anhydride, where a broad peak appeared at −634 ppm which we attribute to $[(VO_2)(TFA)]_2$ species. The difference in chemical shift from this peak to the peak at −545 ppm when this compound is dissolved in D_2O is attributable to solvent effects.[26] When $[Rh(CO)_2Cl]_2$ was added to this solution at room temperature, the color of the solution changed rapidly from orange to green/brown, and the intensity of the ^{51}V peak associated with $[(VO_2)(TFA)]_2$ diminished. Increasing the concentration of Rh(I) caused the peak associated with VO_2^+ to disappear entirely, but no other peaks appeared in the ^{51}V NMR spectrum. The observed change can be attributed to the reaction:

$$Rh(CO)_2(TFA) + [(VO_2)(TFA)]_2 + 4TFAH \rightarrow Rh(CO)_2(TFA)_3 + 2VO(TFA)_2 + 2H_2O$$

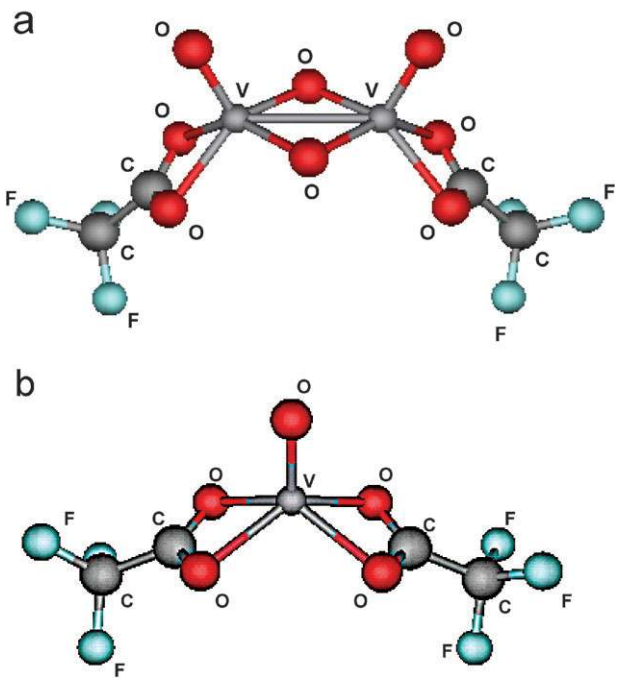

Fig. 9 (a) Computed geometry for $[VO_2(TFA)]_2$. (b) Computed geometry for $VO(TFA)_2$.

The calculated structure for $VO(TFA)_2$ is given in Fig. 9b. The V(IV) species formed as a result of this reaction could not be observed by ^{51}V NMR because of the quadrupolar relaxation of the paramagnetic V(IV) species, which caused the peaks to broaden extensively precluding their detection. The V(IV) species could, however, be observed by UV-visible spectroscopy. Addition of a small quantity of $[Rh(CO)_2Cl]_2$ to a solution containing NH_4VO_3 dissolved in trifluoroacetic acid and water resulted in an immediate color change from orange to blue/green. The resulting UV-visible spectrum is shown in Fig. 11,[2] exhibiting $^2B_{2g} \rightarrow {}^2E_g$, $^2B_{2g} \rightarrow {}^2B_{1g}$, and $^2B_{2g} \rightarrow {}^2A_{1g}$ transitions at 760, 620, and 520 nm, similar to those reported in the literature for VO^{2+} ions upon tetragonal distortion.[27,28] Thus, UV-visible and ^{51}V NMR spectroscopy provide evidence that the active form of the oxidant is VO_2^+, and that this species reduces to VO^{2+} upon oxidation of Rh(I) to Rh(III) *via* the reaction shown above.

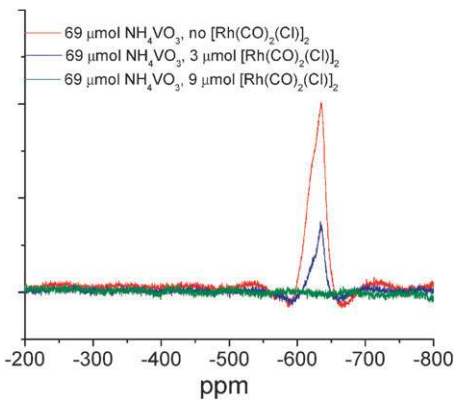

Fig. 10 ^{51}V NMR spectra of NH_4VO_3 (69 μmol) dissolved in TFAH (12.9 mmol).

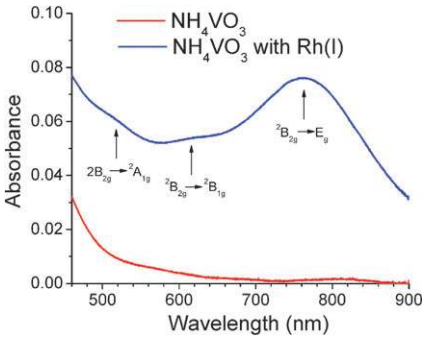

Fig. 11 UV-visible spectrum of a solution of NH_4VO_3 taken before and after addition of Rh(I).

4. Conclusions

Evidence accumulated from experiments and theory provides strong support for the composition and structures of the rhodium and vanadium complexes involved in the mechanism for the oxidative carbonylation of toluene to toluic acid depicted in Scheme 1. The active form of the Rh complex is $Rh(CO)_2(TFA)_3$. The *cis*-positioned carbonyl groups in this complex are found to exhibit unusual interactions with the trifluoroacetate ligands, which give rise to a five-membered ring involving the central rhodium atom. In the course of the reaction, $Rh(CO)_2(TFA)_3$ reduces to $Rh(CO)_2(TFA)$, which, in turn, readily dimerizes to form $[Rh(CO)_2(TFA)]_2$, which exists in equilibrium with the more stable dimer species, $[Rh(CO)_2Cl]_2$. The vanadium species involved in the reoxidation of Rh(I) to Rh(III) (see Scheme 1) is identified as $[VO_2(TFA)]_2$. Reoxidation of Rh(I) by this V(V) species is very rapid and leads to the formation of the paramagnetic species $VO(TFA)_2$.

Acknowledgements

This work was supported by the Methane Conversion Cooperative, funded by BP. A portion of the research was performed using EMSL, a national scientific user facility sponsored by the Department of Energy's Office of Biological and Environmental Research and located at Pacific Northwest National Laboratory.

References and notes

1 I. O. Kalinovskii, A. I. Gel'bshetin and V. V. Pogorelov, *Russ. J. Gen. Chem.*, 2001, **71**, 1463.
2 J. J. Zakzeski and A. T. Bell, *J. Mol. Catal. A: Chem.*, 2007, **276**, 8.
3 A. A. Leshcheva, I. O. Kalinovskii, V. V. Pogorelov, Yu. G. Noskov and A. I. Gel'bshtein, *Kinet. Katal.*, 1998, **39**, 381.
4 I. O. Kalinovskii, Yu. S. Bogachev, A. A. Leshcheva, V. V. Pogorelov, N. N. Shapet'ko and A. I. Gel'bshtein, *Zh. Fiz. Khim.*, 1991, **65**(5), 1404–1406.
5 X. Zheng and A. T. Bell, *J. Phys. Chem. C*, 2008, **112**, 2129.
6 L. Orian, A. Bisello, S. Santi, Al. Ceccon and G. Saielli, *Chem.–Eur. J.*, 2004, **10**, 4029–4040.
7 Y. Shao, L. Fusti-Molnar, Y. Jung, J. Kussmann, C. Ochsenfeld, S. T. Brown, A. T. B. Gilbert, l. V. Slipchenko, S. V. Levchenko, D. P. O'Neill, R. A. Distasio Jr., R. C. Lochan, T. Wang, G. J. O. Beran, N. A. Besley, J. M. Herbert, Y. C. Lin, T. Van Voorhis, S. H. Chien, A. Sodt, R. P. Steele, V. A. Rassolov, P. E. Maslen, P. P. Korambath, R. D. Adamson, B. Austin, J. Baker, E. F. C. Byrd, H. Dachsel, R. J. Doerksen, A. Dreuw, B. D. Dunietz, A. D. Dutoi, T. R. Furlani, S. R. Gwaltney, A. Heyden, S. Hirata,

C. P. Hsu, G. Kedziora, R. Z. Khalliulin, P. Klunzinger, A. M. Lee, M. S. Lee, W. Liang, I. Lotan, N. Nair, B. Peters, E. I. Proynov, P. A. Pieniazek, Y. M. Rhee, J. Ritchie, E. Rosta, C. D. Sherrill, A. C. Simmonett, J. E. Subotnik, H. L. Woodcock III, W. Zhang, A. T. Bell, A. K. Chakraborty, D. M. Chipman, F. J. Keil, A. Warshel, W. J. Hehre, H. F. Schaefer III, J. Kong, A. I. Krylov, P. M. W. Gill and M. Head-Gordon, *Phys. Chem. Chem. Phys.*, 2006, **8**, 3172.
8 A. D. Becke, *J. Chem. Phys.*, 1993, **98**, 5648.
9 C. Lee, W. Yang and R. G. Parr, *Phys. Rev. B: Condens. Matter*, 1998, **37**, 785.
10 P. J. Stephens, F. J. Devlin, C. F. Chabalowski and M. J. Frisch, *J. Phys. Chem.*, 1994, **98**, 11623.
11 A. P. Scott and L. Radom, *J. Phys. Chem.*, 1996, **100**, 16502.
12 L. S. Bresler, N. A. Buzina, Yu. S. Varshavsky, N. V. Kiseleva and T. G. Cherkasova, *J. Organomet. Chem.*, 1979, **171**, 229.
13 P. K. Hurlburt, J. J. Rack, J. S. Luck, S. F. Dec, J. D. Webb, O. P. Anderson and S. H. Strauss, *J. Am. Chem. Soc.*, 1994, **110**, 10002.
14 W. Von Philipsborn, *Pure Appl. Chem.*, 1986, **58**, 513.
15 H.-O. Kalinowsky, S. Berger and S. Braun, *^{13}C NMR Spektroskpie*, Georg Thieme, Verlag, 1984, p. 171.
16 B. Von Ahsen, C. Bach, M. Berkei, M. Köckerling, H. Willner, G. Hägele and F. Aubke, *Inorg. Chem.*, 2003, **42**, 3801.
17 G. Winkhaus and H. Singer, *Chem. Ber.*, 1966, **99**, 3593.
18 B. Botar and P. Koegerler, *Dalton Trans.*, 2008, 3150.
19 B. Botar, P. Koegerler and C. L. Hill, *Inorg. Chem.*, 2007, **46**, 5398.
20 P. A. Chetcuti, J. A. Walker, C. B. Knobler and M. F. Hawthorne, *Organometallics*, 1988, **7**, 641.
21 O. W. Howarth and J. R. Hunt, *J. Chem. Soc., Dalton Trans.*, 1979, 1388.
22 M. J. Little, N. Aubry, M.-E. Beaudoin, N. Goudreau and S. R. LaPlante, *J. Pharm. Biomed. Anal.*, 2007, **43**, 1324.
23 A. Preiß, J. Kruppa, J. Buschmann and C. Mügge, *J. Pharm. Biomed. Anal.*, 1998, **16**, 1381.
24 S. L. T. Andersson, *J. Chem. Soc., Faraday Trans. 1*, 1986, **82**, 1537.
25 D. C. Crans, *Pure Appl. Chem.*, 2005, **77**, 1497.
26 ^{51}V NMR of the vanadium complex indicated a strong interaction with the solvent as indicated by a change in chemical shift when the acid was changed from acetic acid (^{51}V δ = −545 ppm), dichloroacetic acid (^{51}V δ = −574 ppm), chlorodifluoroacetic acid (^{51}V δ = −625 ppm), pentafluoropropionic acid (^{51}V δ = −630 ppm), trifluoroacetic acid (^{51}V δ = −634 ppm), methanesulfonic acid (^{51}V δ = −685 ppm).
27 Ch. Linga Raju, K. V. Narasimhulu, N. O. Gopal, J. L. Rao and B. C. V. Reddy, *J. Mol. Struct.*, 2005, **754**, 100.
28 N. Satyanarayana, *Spectrochim. Acta, Part A*, 1985, **41**, 1185.
29 J. Zakzeski, A. Behn, M. Head-Gordon and A. T. Bell, *J. Am. Chem. Soc.*, 2009, **131**, 11098.